

## SUPPORTING INFORMATION

### Structure-based optimization of ML300 derived, non-covalent inhibitors targeting the severe acute respiratory syndrome coronavirus 3CL protease (SARS-CoV-2 3CL<sup>pro</sup>)

Sang Hoon Han<sup>a</sup>, Christopher M. Goins<sup>a</sup>, Tarun Arya<sup>a</sup>, Woo-Jin Shin<sup>b</sup>, Joshua Maw<sup>a</sup>, Alice Hooper<sup>a</sup>, Dhiraj P. Sonawane<sup>a</sup>, Matthew R. Porter<sup>a</sup>, Breyanne E. Bannister<sup>c</sup>, Rachel D. Crouch<sup>c</sup>, A. Abigail Lindsey<sup>a</sup>, Gabriella Lakatos<sup>a</sup>, Steven R. Martinez<sup>a</sup>, Joseph Alvarado<sup>a</sup>, Wendell S. Akers<sup>c</sup>, Nancy S. Wang<sup>a</sup>, Jae U. Jung<sup>d,e</sup>, Jonathan D. Macdonald<sup>a</sup>, Shaun R. Stauffer<sup>a\*</sup>

<sup>a</sup>Center for Therapeutics Discovery, Lerner Research Institute, Cleveland Clinic, Cleveland, OH, 44195, USA

<sup>b</sup>Cleveland Clinic Florida Research & Innovation Center, Port St. Lucie, FL, 34987, USA

<sup>c</sup>Department of Pharmaceutical Science, Lipscomb University College of Pharmacy, Nashville, TN, 37204, USA

<sup>d</sup>Department of Cancer Biology, Lerner Research Institute, Cleveland Clinic, Cleveland, OH, 44195, USA

<sup>e</sup>Center for Global and Emerging Pathogens Research, Lerner Research Institute, Cleveland Clinic, Cleveland, OH, 44195, USA

\*Corresponding author, Email: [stauffss2@ccf.org](mailto:stauffss2@ccf.org)

#### Table of Contents

##### *Supplemental Data*

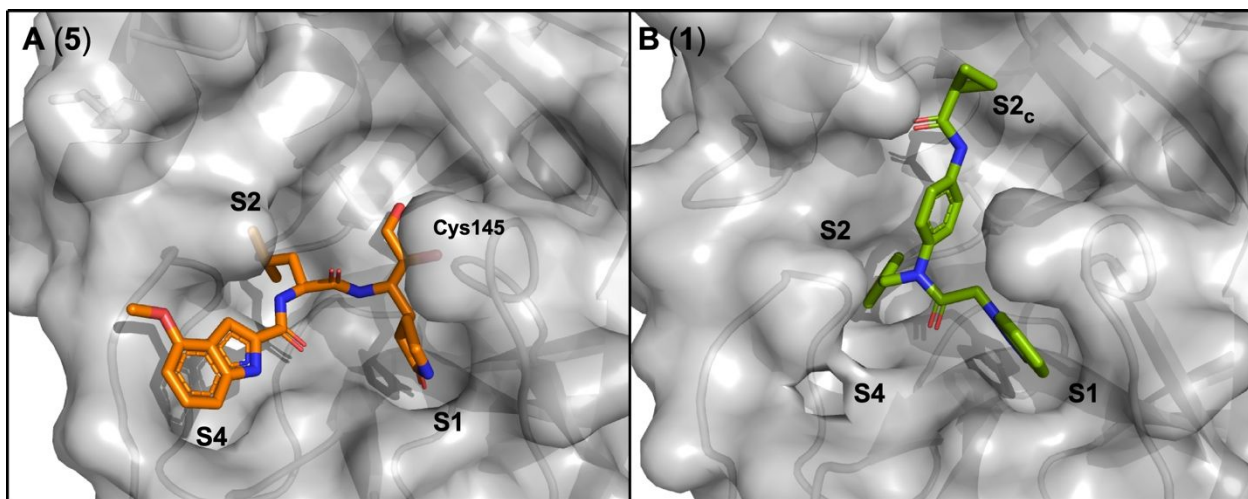
Figure S1. Comparison of SARS-CoV-2 3CL <sup>pro</sup> X-ray crystal structures of <b>1</b> and <b>5</b>	S2
Figure S2. SARS-CoV-1 3CL <sup>pro</sup> X-ray crystal structures of <b>19</b> , <b>21</b> , <b>35</b>	S2
Table S1. Tier 1 DMPK Summary	S3
Table S2. Fragmentation of <b>36</b> and proposed metabolites in Human S9	S4

##### *Structural Biology Experimental Details*

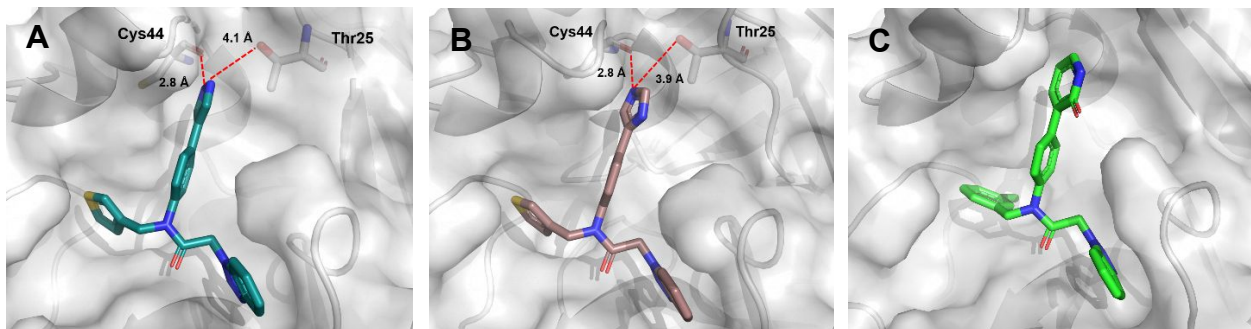
Table S3. SARS CoV-2 3CL <sup>pro</sup> X-ray Data Collection and Refinement Statistics.	S5
Table S4. SARS-CoV-1 3CL <sup>pro</sup> X-ray Data Collection and Refinement Statistics.	S6
Figure S3. Ligand electron density maps	S7

##### *Compound HPLC Traces*

VeroE6 CPE SARS-CoV-2 antiviral activity data compound <b>41</b>	S19
Figure S4. Concentration-response-curve	S19
Table S5. CPE Vero E6 infected cells % viability raw data	S19



**Supplemental Figure S1.** Comparison of 3CL<sup>pro</sup> main binding site when bound to covalent inhibitor **5**, and this series lead, **1**. The two molecules have significantly different binding poses, occupying alternate regions of the enzyme binding pocket. **A** – Published X-ray co-crystal structure of **5** – SARS-CoV-2 3CL<sup>pro</sup> (PDB: 6XHM); **B** – X-ray co-crystal structure of **1** (ML300) bound to SARS-CoV-2 3CL<sup>pro</sup> (PDB: 7LME).



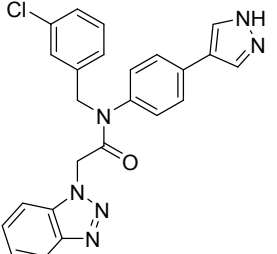
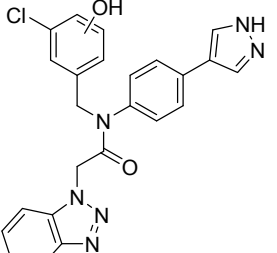
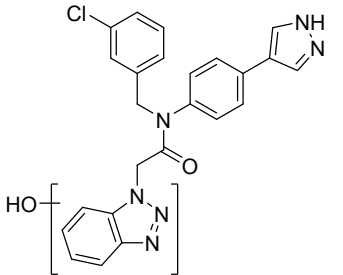
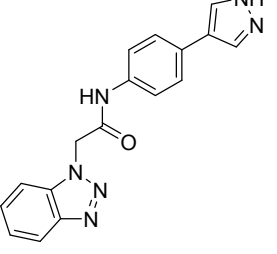
**Supplemental Figure S2.** X-ray crystal structures of SARS-CoV-1 3CL<sup>pro</sup> in complex with compounds, **19** (A), **21** (B), and **35** (C). All structures were generated by soaking apo-crystals with compound DMSO stock, and via this methodology we observe a glycerol molecule (not shown) in each structure in the S4 region.

**Supplemental Table S1.** Summary of tier 1 DMPK data.

Cmpd.	HLM <sup>a</sup>		Human S9		RLM <sup>b</sup>		PPB, F <sub>u</sub> (%) <sup>c</sup>		MDCK <sup>d</sup>	CYP Profile (% Inh. at 10 μM) <sup>e</sup>		
	t <sub>1/2</sub> (min)	CL <sub>int'</sub> (mL/min/kg)	CL <sub>int'</sub> (mL/min/kg)	CL <sub>hep</sub> (mL/min/kg)	t <sub>1/2</sub> (min)	CL <sub>int'</sub> (mL/min/kg)	Human Plasma	Rat Plasma	P <sub>app</sub> [A-B] (x10 <sup>-6</sup> cm/s)	3A4	2D6	2C9
<b>8</b>	2.0	1263.5			*	-	0.62%	**	80	85.7	44.8	63.4
<b>19</b>	1.7	1465.1			2.6	1995	0.35%	**	59.8	95.8	61.9	98.0
<b>21</b>	16.8	168			10.0	553	1.7%	**	33	98.8	80	99
<b>25</b>	1.1	2378.4			*	-	0.25%	2.20%	81	89.6	45.5	72.3
<b>27</b>	19.1	125.3			2.2	2568	2.41%	23.00%	71.6	64.0	18.3	1.7
<b>28</b>	*	-			*	-	0.20%	0.74%	55	92.8	79.5	89.5
<b>31</b>	*	-			*	-	0.24%	0.75%	59.5	93.3	82.9	89.2
<b>33</b>	*	-			*	-	0.07%	0.29%	24	95.6	82.0	84.7
<b>34</b>	2.6	1080			*	-	0.8%	5.3%	66.9	95.4	67	59
<b>35</b>	4.4	574.9			1.6	3461	1.42%	0.48%	43.8	69.6	22.6	75.0
<b>36</b>	1.0	2621	436	20	1.0	5668	0.1%	**	39.4	96	63	99
<b>38</b>	1.0	2496			1.0	5525	<0.06%	0.8%	20.9	97.1	69	100
<b>39</b>	1.2	2036			*	-	0.9%	6.1%	46.7	92.0	44	89
<b>40</b>	1.2	2175.2	471	20.1	*	-	0.2%	5.6%	61.8	94.1	42	97
<b>41</b>	21.1	141			12.3	589	0.7%	1.8%	46.1	100	87.2	100
<b>42</b>	2.5	980.7	256	19.4	1.6	3555	0.4%	3.5%	61.8	99	55	98.5
<b>43</b>	4.1	620.4	145	18.3	1.7	3302	1.8%	11.0%	66.7	87.7	25.7	91.9

Tier 1 DMPK generated at Q2 solutions, except hS9 data generated at Lipscomb University College of Pharmacy. <sup>a</sup>HLM – Human liver microsomes; <sup>b</sup>RLM – Rat liver microsomes; <sup>c</sup>F<sub>u</sub> – Fraction Unbound; <sup>d</sup>Permeability in MDCK-MDR1 cells; <sup>e</sup>CYP % inhibition at 10 μM; \* – Rapid clearance, not reliably measured; \*\* – Low compound recovery

**Supplemental Table S2.** Fragmentation of compound **36** and proposed metabolites in Human S9.

Metabolite	Structure	[M+H] <sup>+</sup>	Fragment Ions
<b>36</b> Parent		443	326, 134, 127, 118
<b>M1</b> <sup>a</sup> 60% of total metabolite peak area		459	301, 202, 174, 143
<b>M2</b> 33% of total metabolite peak area		459	326, 151, 127
<b>M3</b> 7% of total metabolite peak area		319	202, 186, 174, 119

<sup>a</sup> Metabolite formation (%) based on the total peak area (total peak AUC) of the three principle metabolites, M1, M2 and M3.

## Structural Biology Experimental Details

**Supplemental Table S3.** SARS-CoV-2 3CL<sup>pro</sup> X-ray refinement statistics. One crystal was used for each structure. Values in parentheses unless stated represent data in the highest-resolution shell. RMS = Root mean square

Compound	1 7LME	19 7LMD	21 7LMF
<b>Data Collection</b>			
Beamline	APS 21-ID-F	APS 21-ID-F	APS 21-ID-F
Wavelength (Å)	0.978	0.978	0.978
Resolution range (Å)	43.72–2.10 (2.18–2.10)	24.49–1.96 (2.03–1.96)	43.75–2.20 (2.28–2.20)
Space group	P 1 21 1	C 1 2 1	P 1 21 1
Unit cell			
a, b, c (Å)	44.45, 53.75, 114.18	115.16, 54.34, 44.45	44.54, 53.70, 114.75
α, β, γ (°)	90, 101.98, 90	90, 101.01, 90	90, 100.80, 90
Total reflections	227385	61969	204060
Unique reflections	30873 (3016)	19327 (1911)	27231 (2691)
Multiplicity	7.4 (5.9)	3.2 (3.0)	7.5 (6.9)
Completeness (%)	99.16 (94.27)	98.68 (98.25)	99.53 (96.93)
Mean I/σI	15.57 (1.95)	31.63 (6.77)	19.00 (2.37)
Wilson B-factor	26.18	23.99	29.82
R-merge	0.139 (0.831)	0.066 (0.237)	0.126 (0.793)
R-meas	0.149 (0.910)	0.079 (0.288)	0.135 (0.857)
R-pim	0.054 (0.366)	0.043 (0.162)	0.049 (0.322)
CC1/2	0.996 (0.705)	0.994 (0.901)	0.995 (0.793)
<b>Structure Refinement</b>			
Reflections used in refinement	30823 (2928)	19326 (1911)	27179 (2623)
Reflections used for R-free	1481 (143)	960 (78)	1384 (116)
R-work	0.1802 (0.2292)	0.1878 (0.2261)	0.1857 (0.2307)
R-free	0.2405 (0.2870)	0.2340 (0.2919)	0.2539 (0.3330)
Number of non-hydrogen atoms	4975	2580	4912
macromolecules	4673	2333	4704
ligands	62	30	60
solvent	240	217	148
Protein residues	609	302	610
RMS (bonds)	0.007	0.007	0.007
RMS (angles)	0.84	0.89	0.91
Ramachandran favored (%)	98.35	98.00	96.20
Ramachandran allowed (%)	1.49	2.00	3.30
Ramachandran outliers (%)	0.17	0	0.50
Rotamer outliers (%)	0	0	0
Clash score	3.68	3.66	3.95
Average B-factor	28.60	27.08	33.22
macromolecules	28.33	26.70	33.10
ligands	36.2	30.74	40.36
solvent	31.8	30.63	34.2

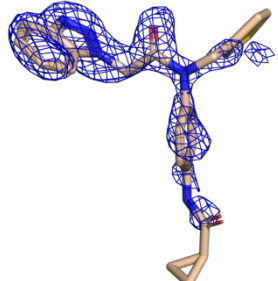
**Supplemental Table S4.** SARS-CoV-1 3CL<sup>pro</sup> X-ray refinement statistics. One crystal was used for each structure. Values in parentheses unless stated represent data in the highest-resolution shell. RMS = Root mean square

Compound	8 7LMH	19 7LMI	21 7LMG	35 7LMJ
<b>PDB Accession Code</b>				
Beamline	APS 21-ID-F	APS 21-ID-F	APS 21-ID-F	APS 21-ID-F
Wavelength (Å)	0.978	0.978	0.978	0.978
Resolution range (Å)	32.30 - 1.85 (1.92 - 1.85)	32.34 - 1.71 (1.77 - 1.71)	32.33 - 1.69 (1.75 - 1.69)	32.06 - 1.60 (1.66 - 1.60)
Space group	C 1 2 1	C 1 2 1	C 1 2 1	C 1 2 1
Unit cell				
a, b, c (Å)	107.69 82.47 53.30	108.51 82.11 53.38	107.54 82.71 53.20	108.41 81.82 53.36
α, β, γ (°)	90 105.2 90	90 104.7 90	90 105.3 90	90 104.7 90
Total reflections	76397	97473	99960	114896
Unique reflections	38216 (3632)	48839 (4776)	50018 (4788)	57645 (5434)
Multiplicity	7.6 (7.4)	7.6 (7.4)	7.6 (7.4)	7.6 (7.4)
Completeness (%)	99.42 (94.90)	99.75 (98.09)	99.50 (95.68)	96.98 (90.93)
Mean I/σI	22.31 (7.90)	10.76 (2.59)	17.06 (2.73)	7.38 (3.20)
Wilson B-factor	32.29	28.83	32.53	23.62
R-merge	0.019 (0.092)	0.055 (0.322)	0.030 (0.242)	0.085 (0.277)
R-meas	0.027 (0.130)	0.077 (0.455)	0.042 (0.342)	0.120 (0.392)
R-pim	0.019 (0.092)	0.055 (0.322)	0.030 (0.242)	0.085 (0.277)
CC1/2	0.999 (0.985)	0.987 (0.834)	0.995 (0.923)	0.99 (0.97)
<b>Structure Refinement</b>				
Reflections used in refinement	38200 (3632)	48829 (4773)	50015 (4788)	57604 (5426)
Reflections used for R-free	1903 (165)	2448 (269)	2502 (253)	2896 (299)
R-work	0.1540 (0.1797)	0.1957 (0.3025)	0.1928 (0.2935)	0.1968 (0.2418)
R-free	0.2004 (0.2878)	0.2094 (0.3297)	0.2216 (0.2963)	0.2345 (0.2909)
Number of non-hydrogen atoms	2709	2675	2757	2567
macromolecules	2393	2420	2390	2401
ligands	43	42	66	36
solvent	273	213	301	130
Protein residues	306	306	306	306
RMS (bonds)	0.018	0.016	0.015	0.019
RMS (angles)	2.13	2.03	1.96	2.17
Ramachandran favored (%)	97.37	97.37	98.68	97.37
Ramachandran allowed (%)	2.63	2.63	1.32	2.63
Ramachandran outliers (%)	0	0	0	0
Rotamer outliers (%)	3.76	2.95	1.13	2.62
Clash score	3.96	4.31	13.01	2.29
Average B-factor	38.61	34.62	41.22	28.53
macromolecules	37.43	33.83	39.04	28.33
ligands	43.22	39.88	45.30	28.18
solvent	48.22	42.60	57.70	32.34

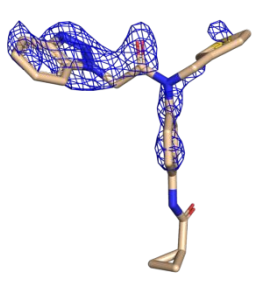
**Supplemental Figure S3.** SARS-CoV-1 and CoV-2 3CL<sup>pro</sup> F<sub>o</sub>-F<sub>c</sub> likelihood-weighted omit maps for ligands, with respective sigma contours given:

**A:** SARS-CoV-2 3CL<sup>pro</sup> in complex with compound **1** (PDB:7LME)

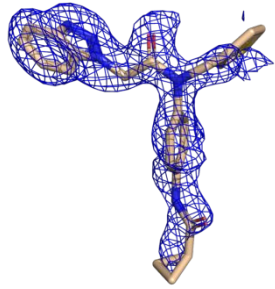
Ligand in Chain A, ! = 3.0



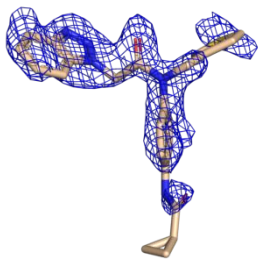
Ligand in Chain B, ! = 3.0



Ligand in Chain A, ! = 2.0

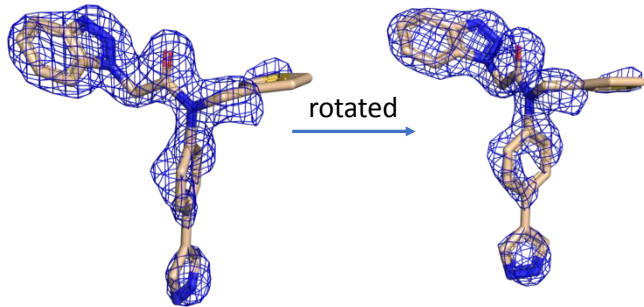


Ligand in Chain B, ! = 2.0



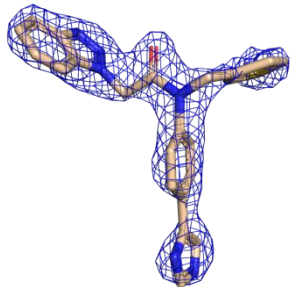
**B:** SARS-CoV-2 3CL<sup>pro</sup> in complex with compound **19** (PDB:7LMD)

Ligand in Chain A, ! = 3.0

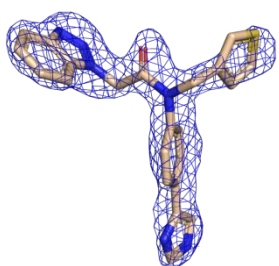


C: SARS-CoV-2 3CL<sup>pro</sup> in complex with compound **21** (PDB: 7LMF)

Ligand in Chain A, ! = 3.0

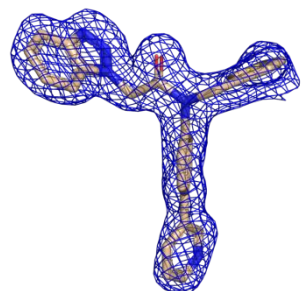


Ligand in Chain B, ! = 3.0



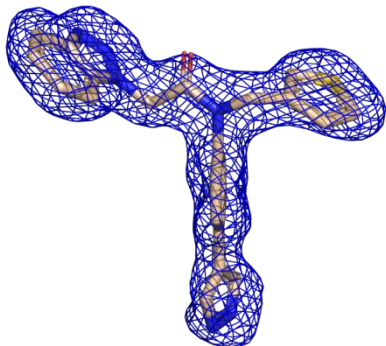
D: SARS-CoV-1 3CL<sup>pro</sup> in complex with compound **8** (PDB: 7LMH)

Ligand in Chain A, ! = 3.0



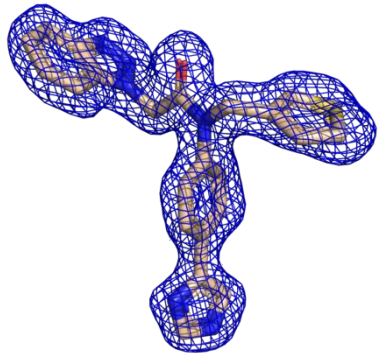
E: SARS-CoV-1 3CL<sup>pro</sup> in complex with compound **19** (PDB: 7LMI)

Ligand in Chain A, ! = 3.0



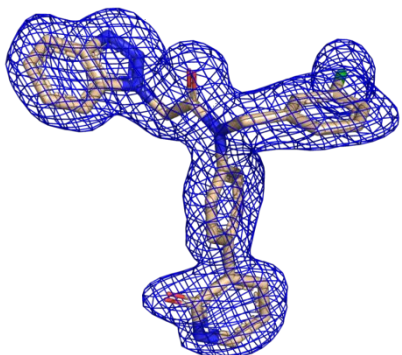
F: SARS-CoV-1 3CL<sup>pro</sup> in complex with compound **21** (PDB: 7LMG)

Ligand in Chain A, ! = 3.0



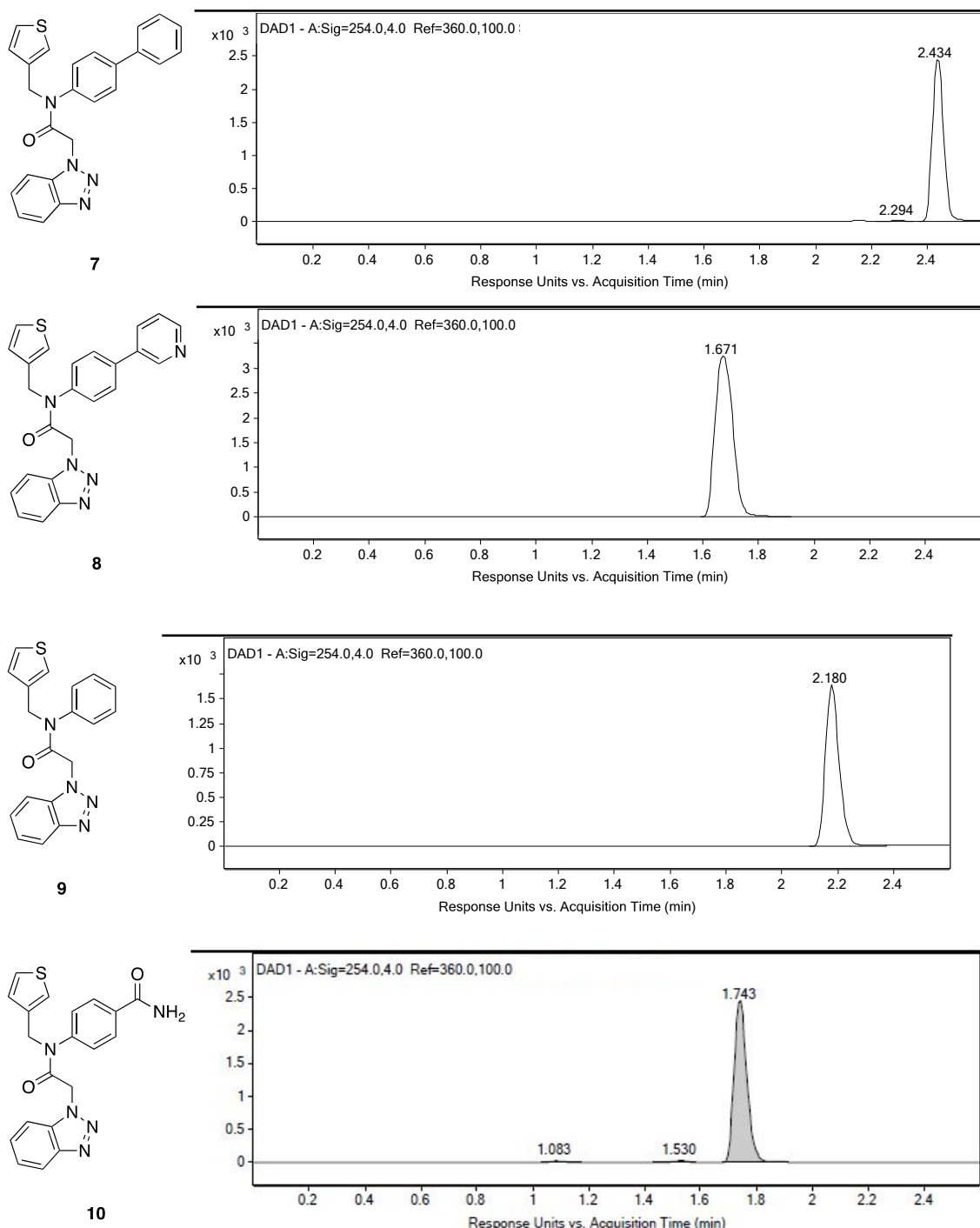
G: SARS-CoV-1 3CL<sup>pro</sup> in complex with compound **35** (PDB: 7LMJ)

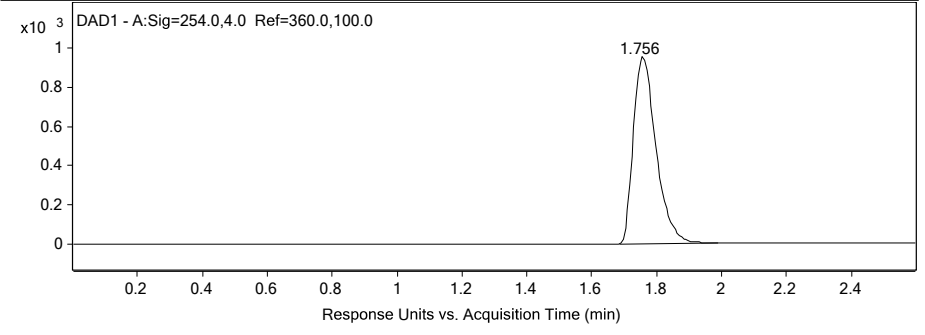
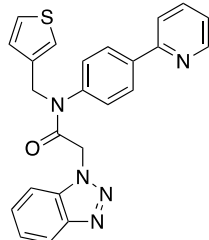
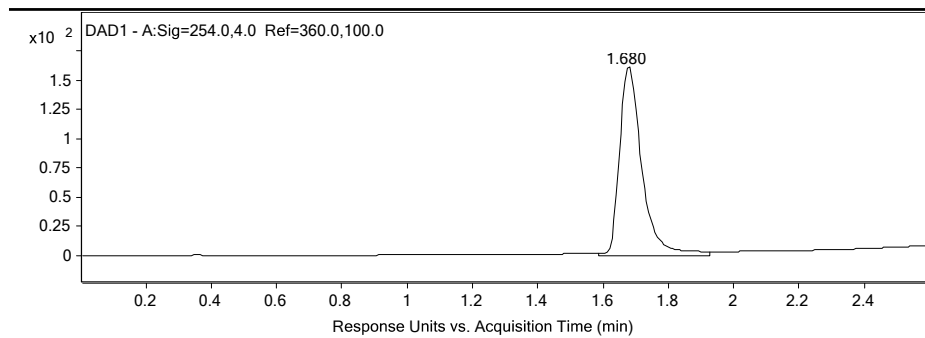
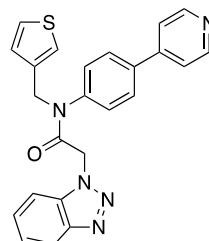
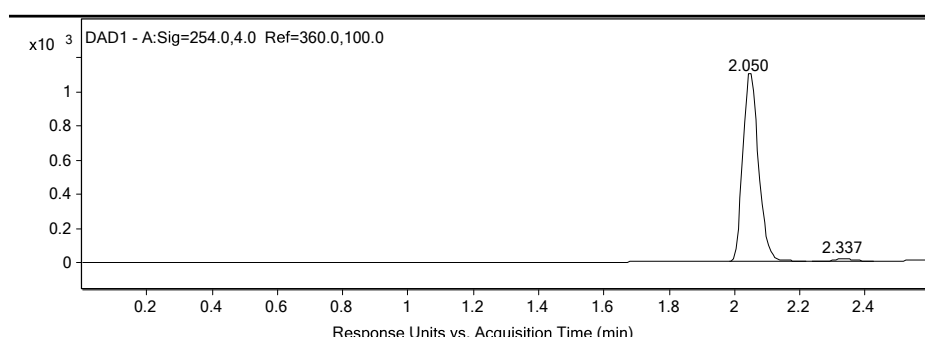
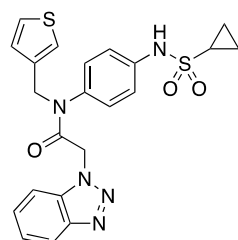
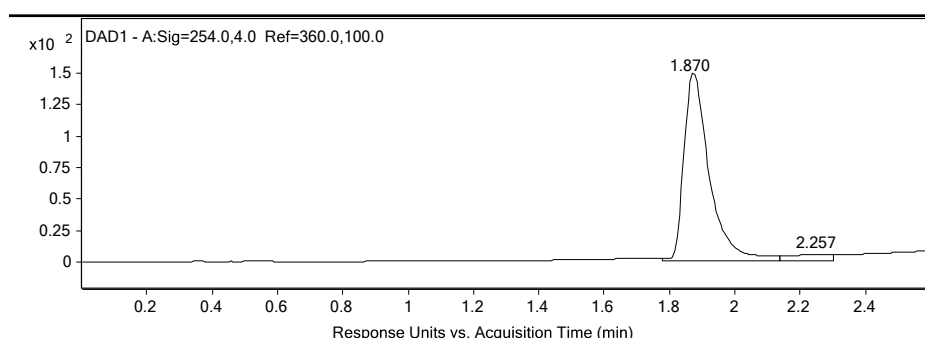
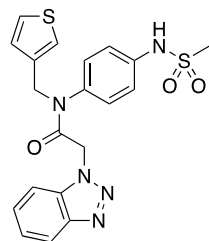
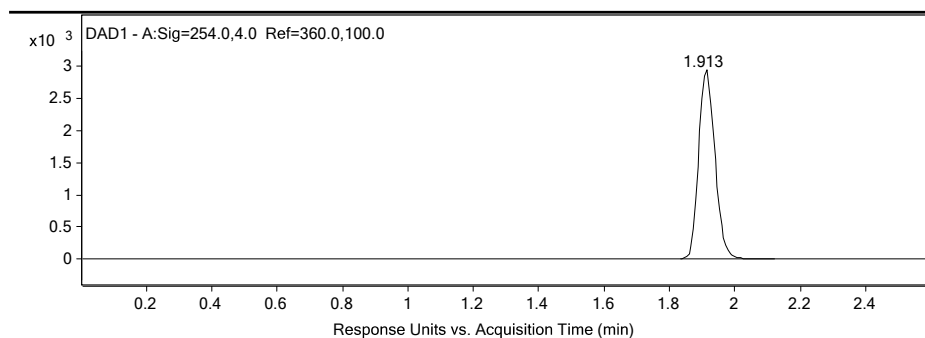
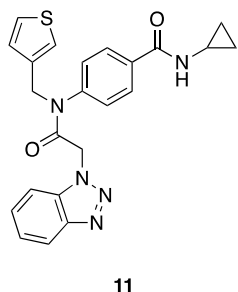
Ligand in Chain A, ! = 3.0

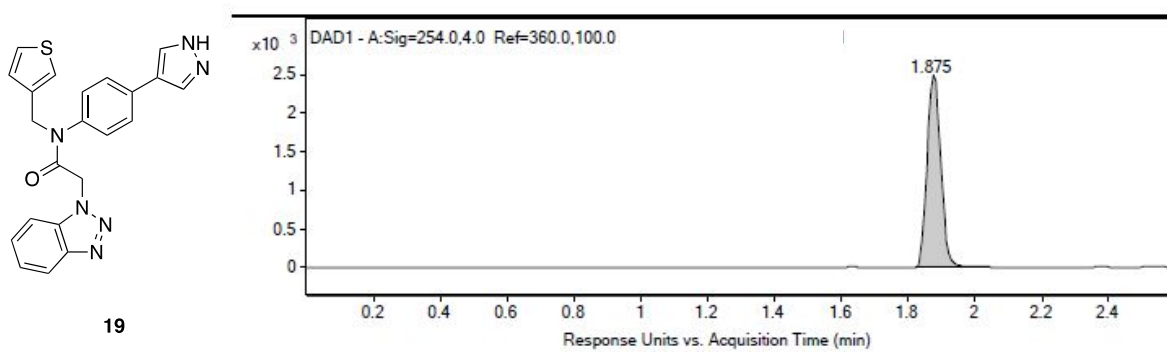
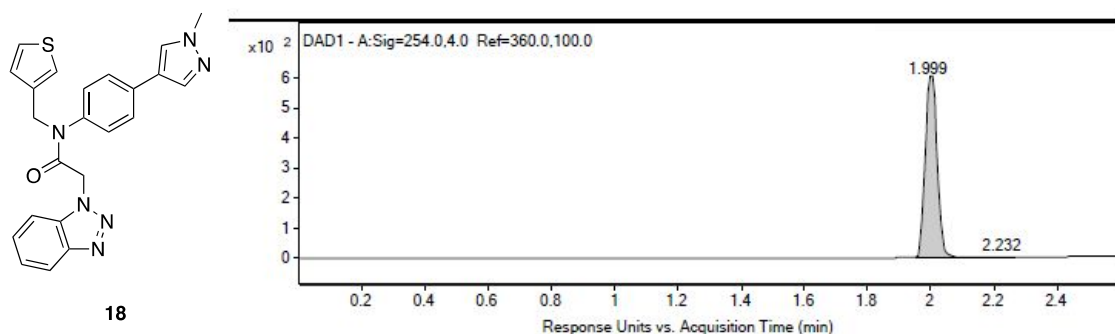
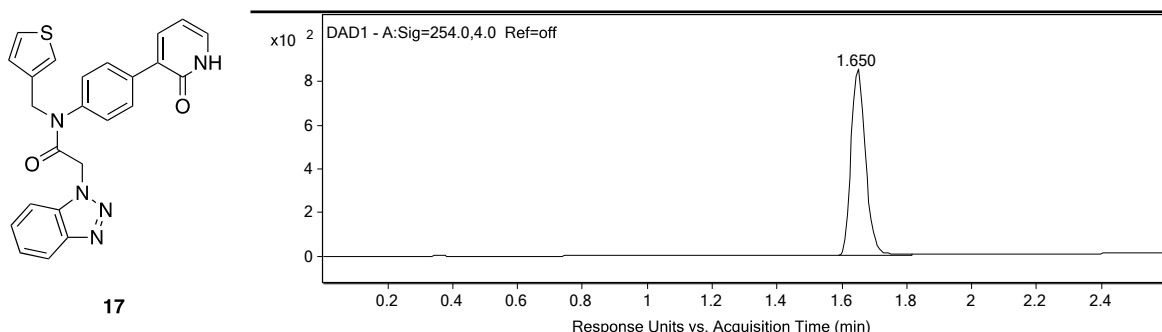
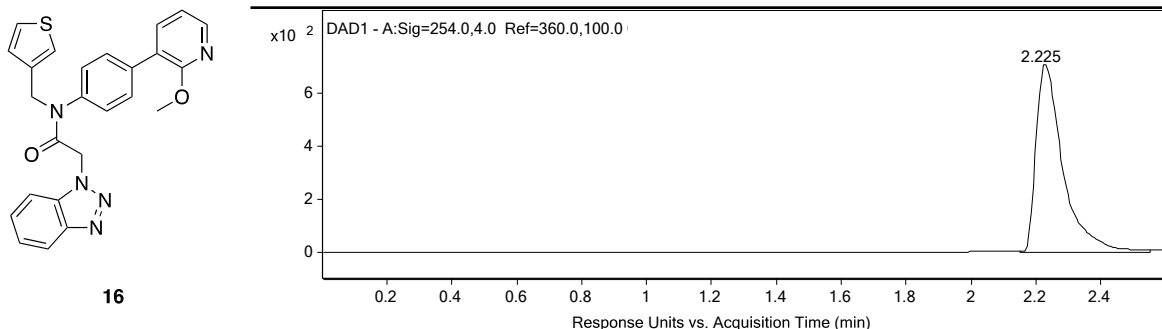


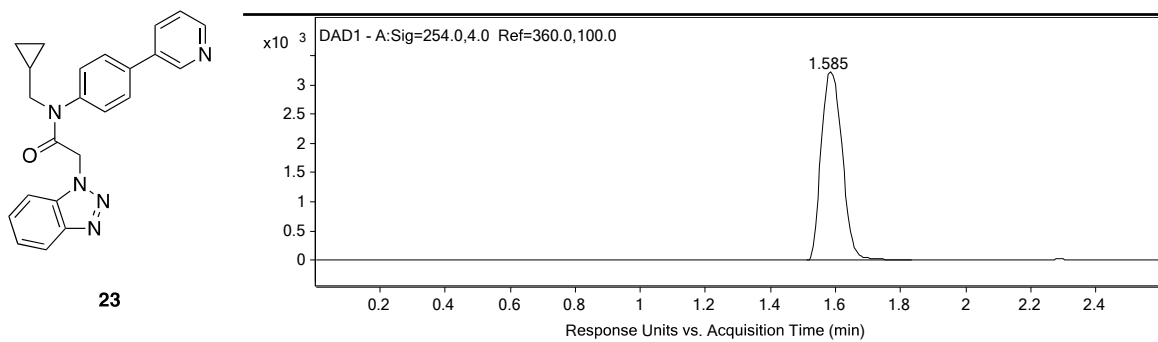
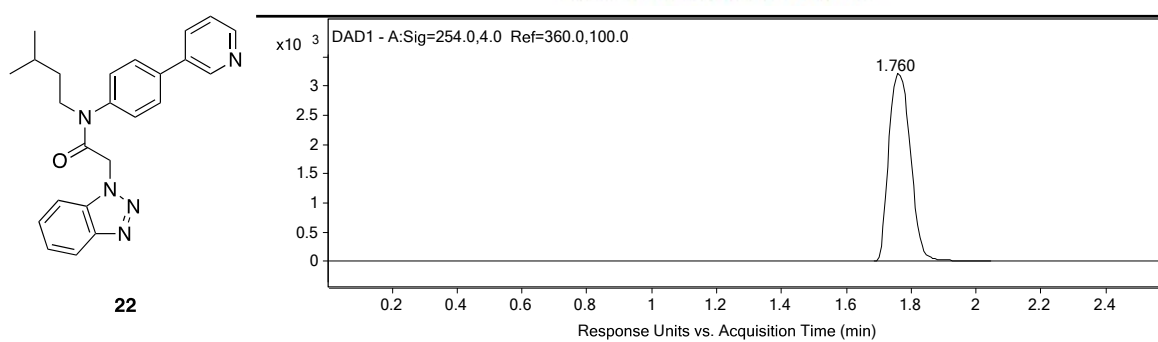
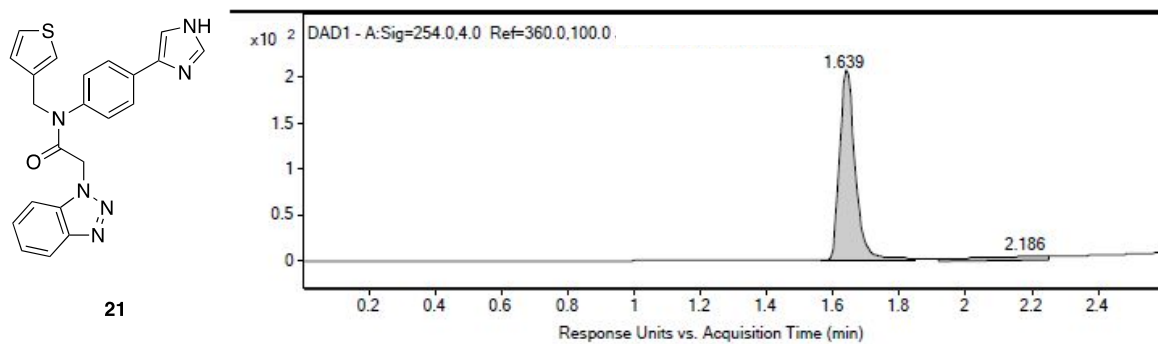
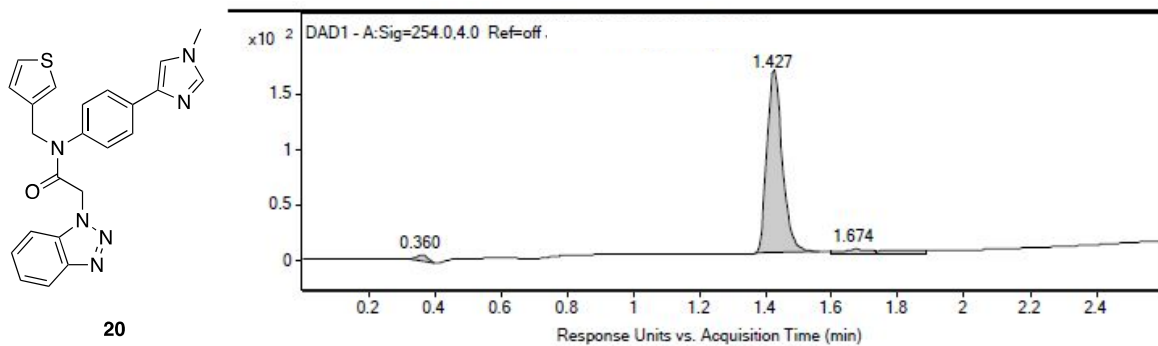
## Compound HPLC Traces

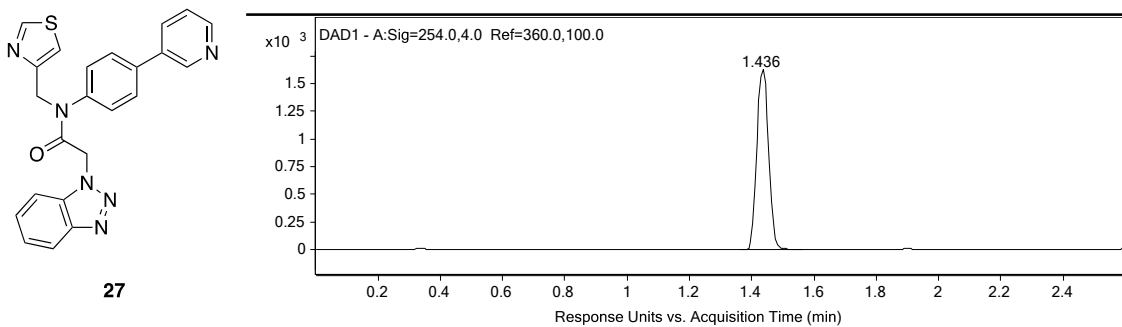
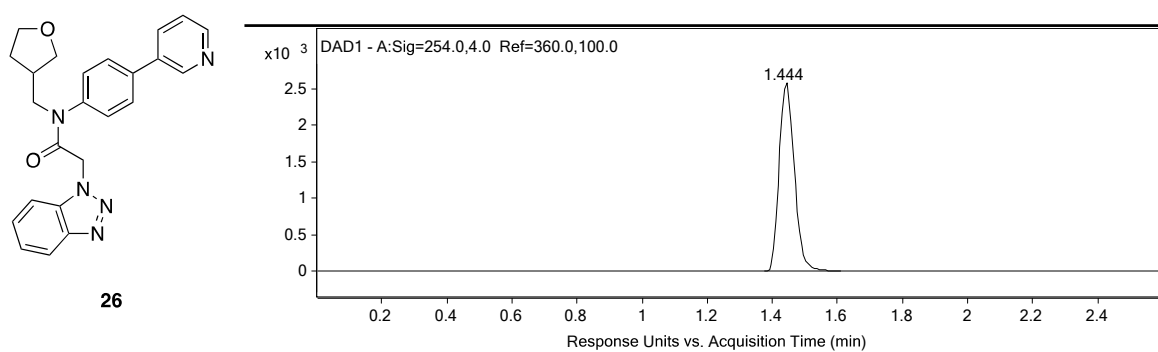
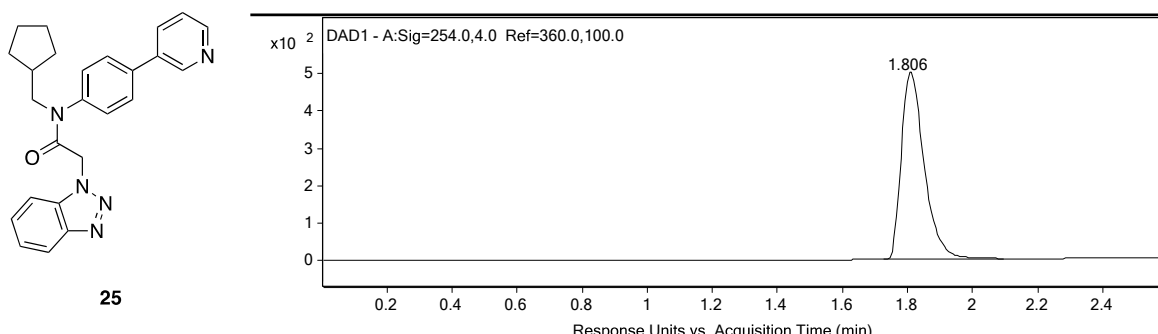
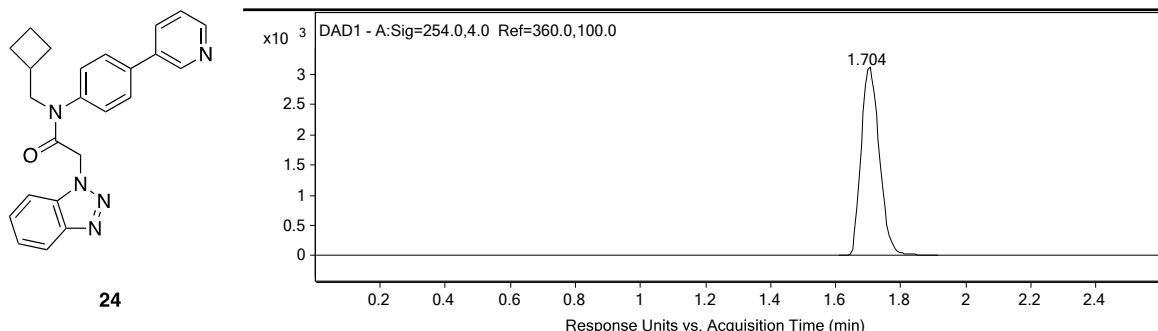
LCMS Method A (see main manuscript) – shown are UV traces @ 254 nm

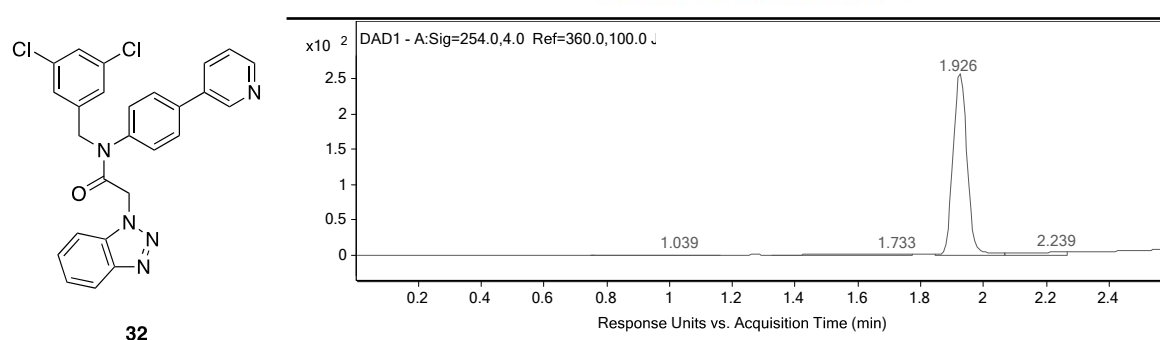
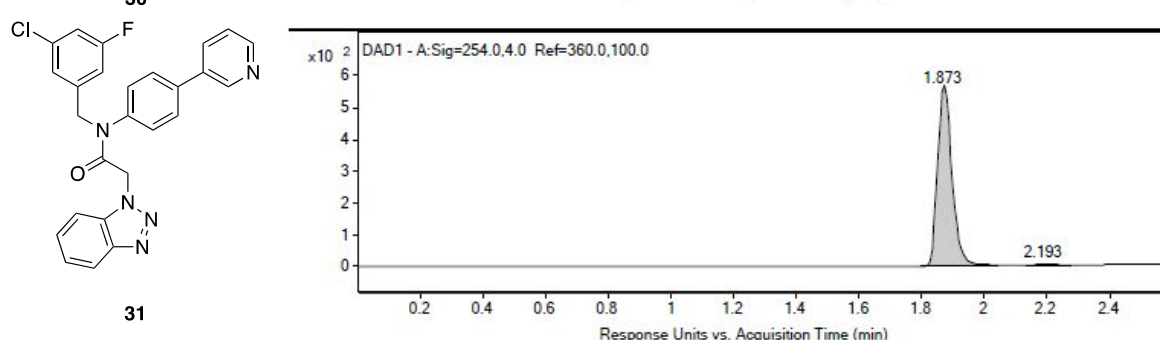
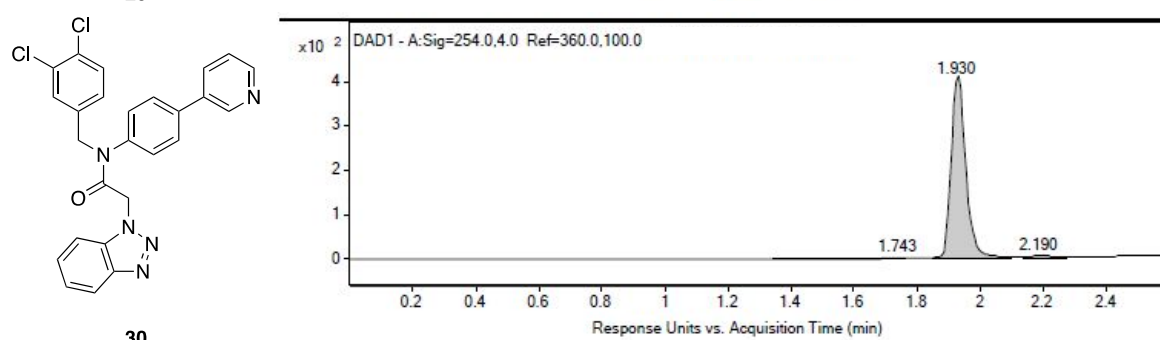
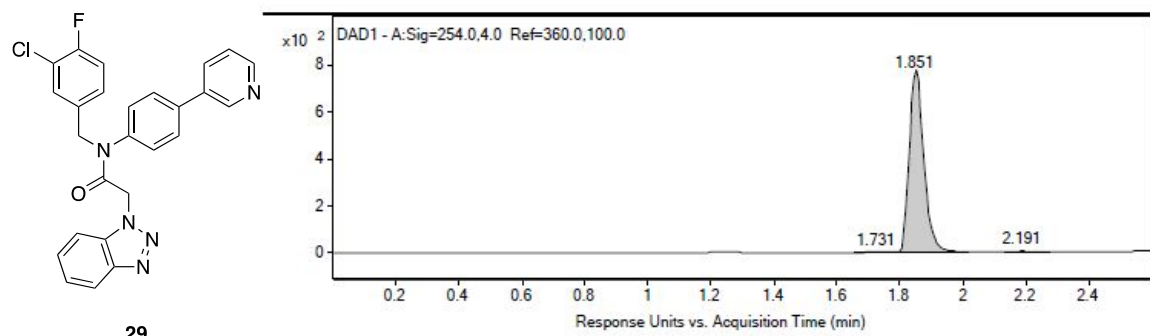
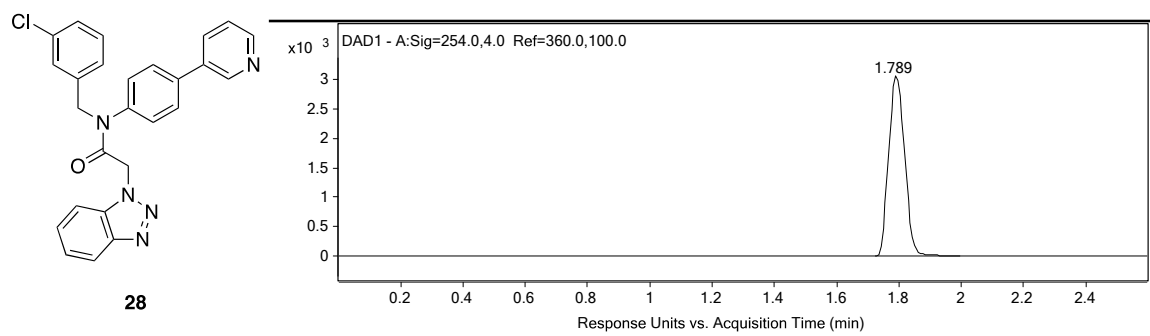


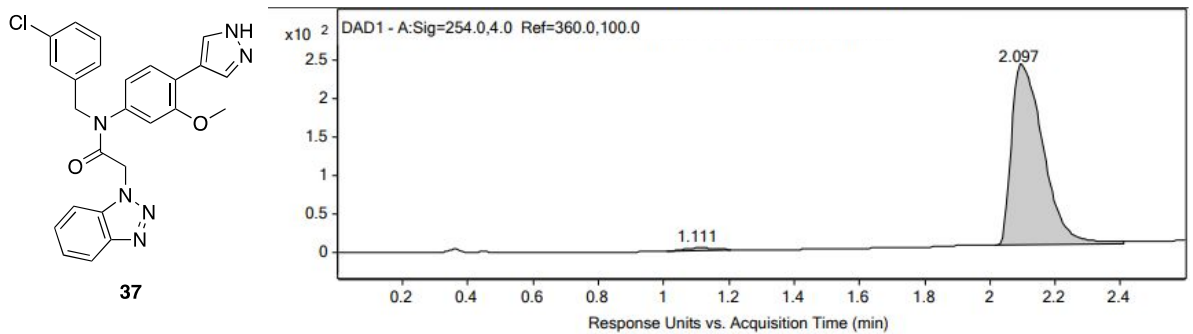
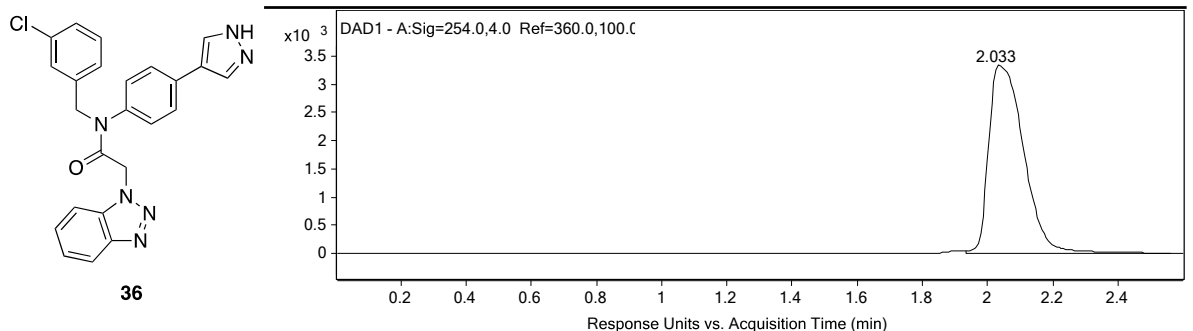
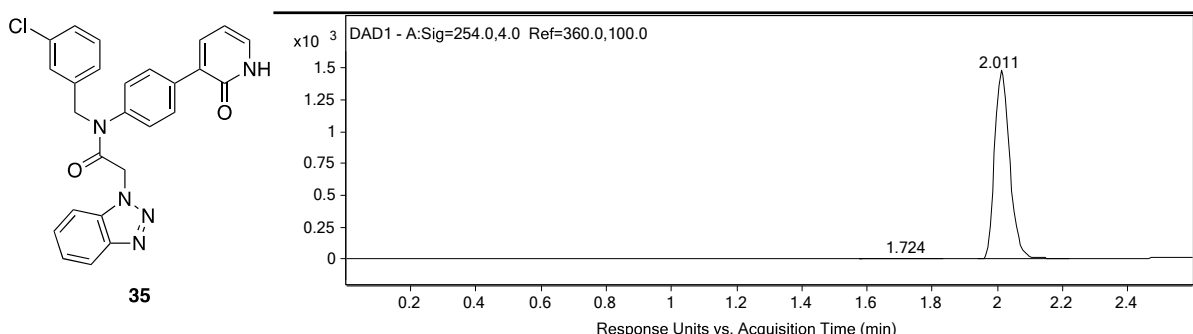
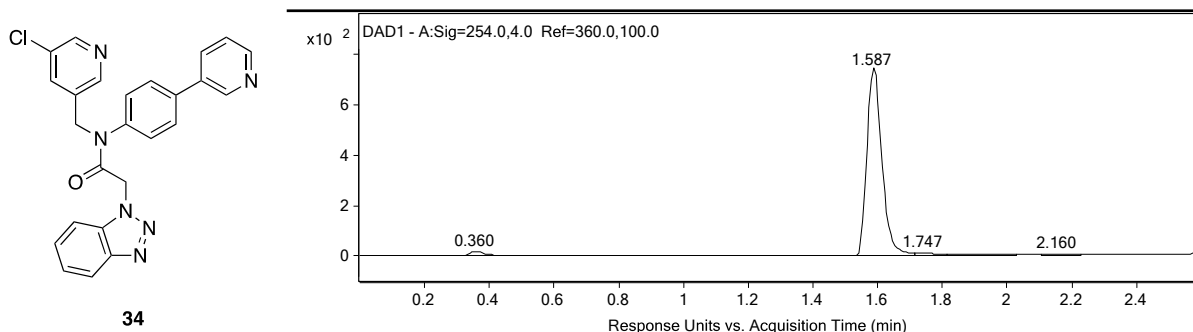
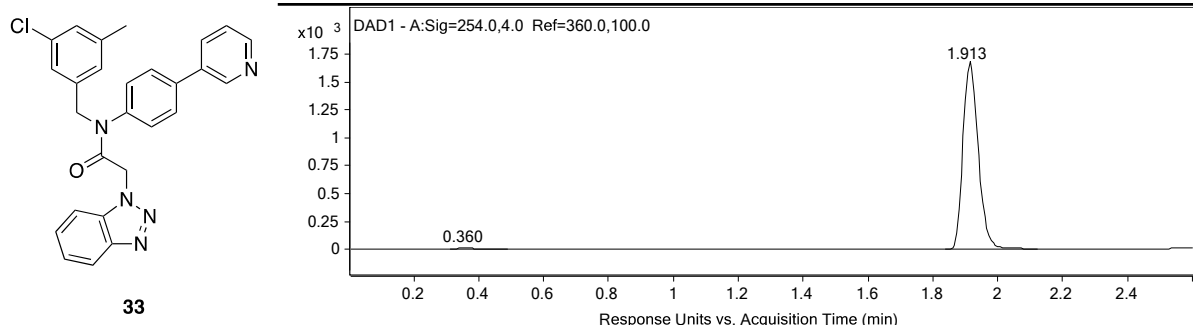


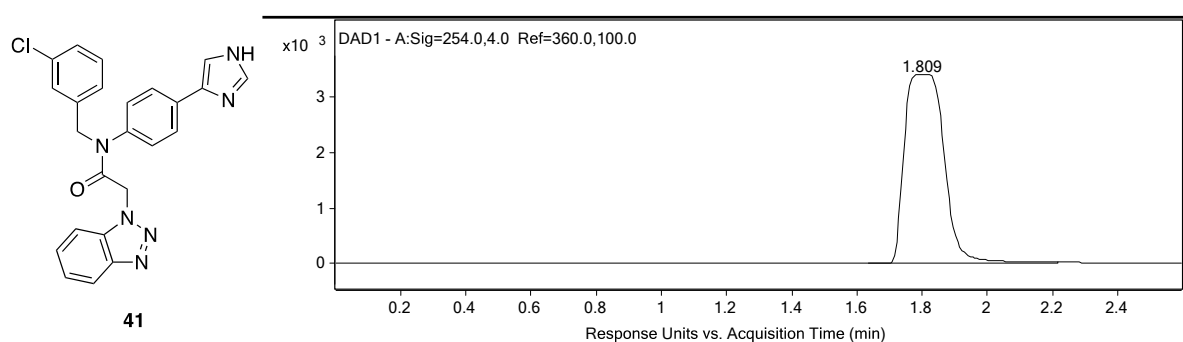
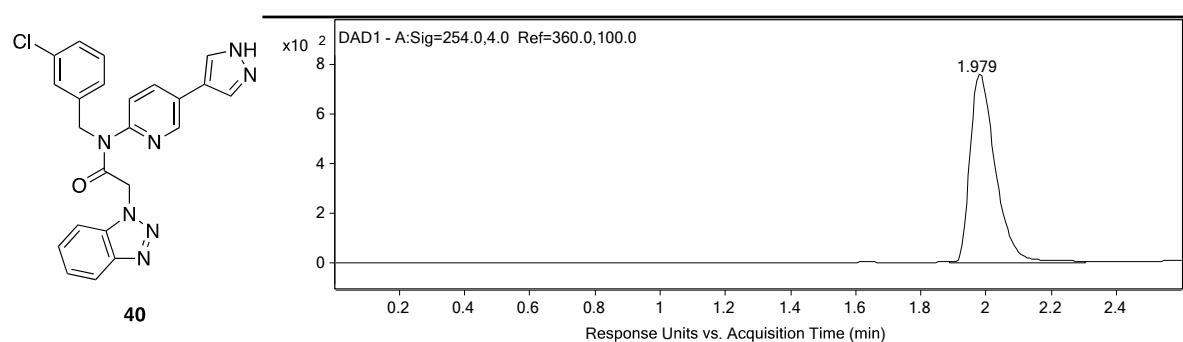
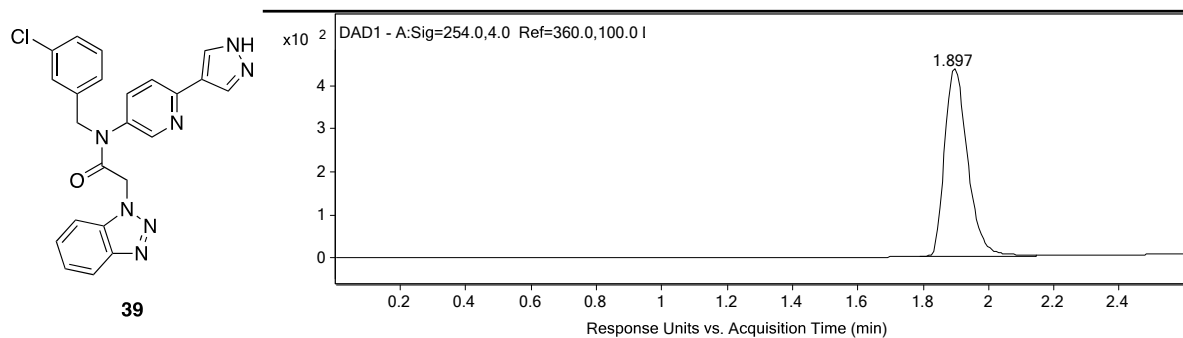
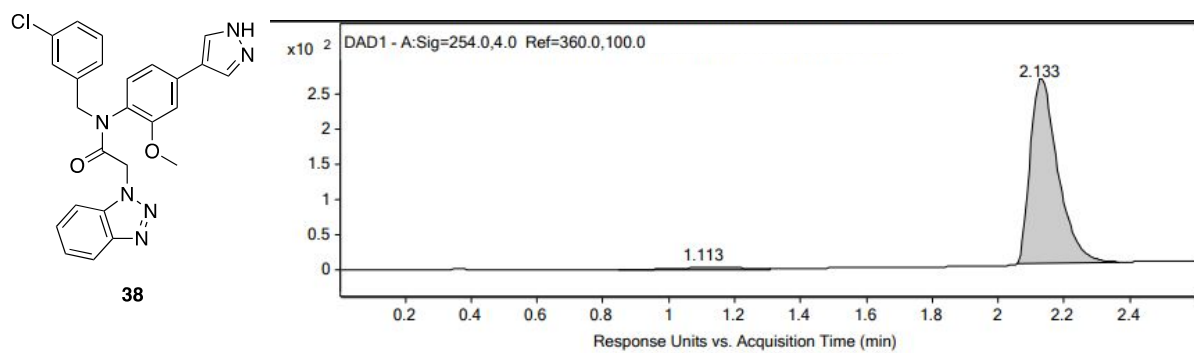


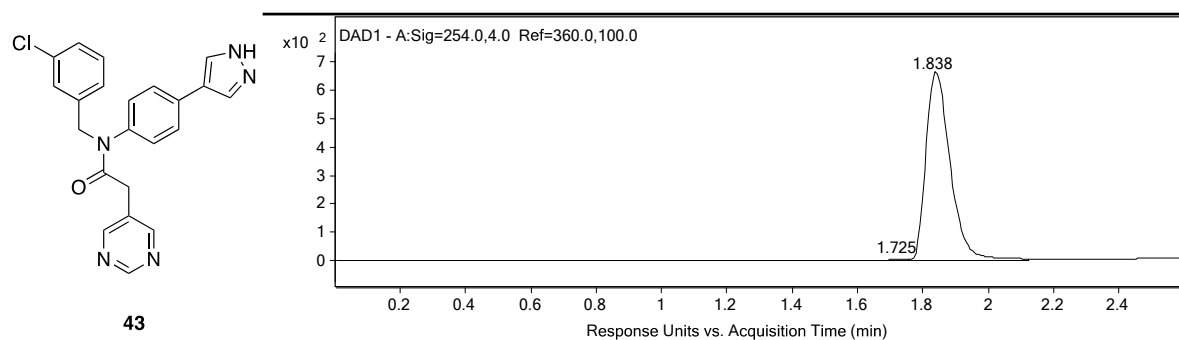
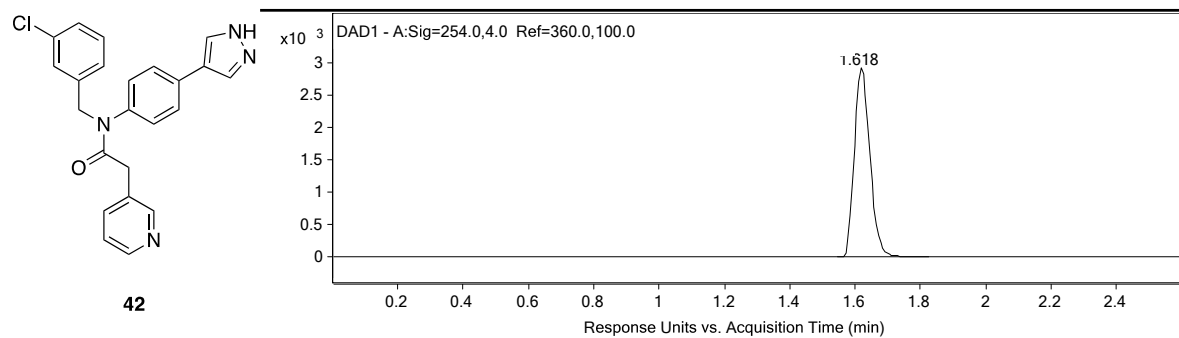




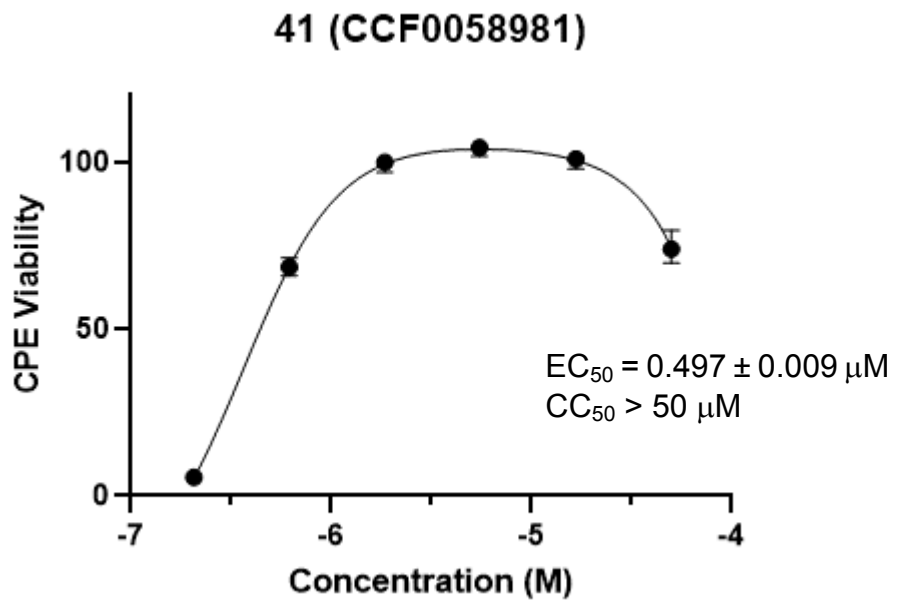








**Supplemental Figure S4.** SARS-CoV-2 Vero E6 CPE Viability CRC **41**



**Supplemental Table S5.** Viability SARS-CoV-2 mock-infected Vero E6 cells using **41**.

[41] % Viability	50 $\mu M$	16.6 $\mu M$	5.55 $\mu M$	1.85 $\mu M$	0.617 $\mu M$	0.206 $\mu M$
	69.77	102.59	105.33	99.96	65.91	6.61
	79.50	97.90	104.39	101.21	71.29	3.49
	73.91	100.96	101.78	96.94	68.53	5.50